Supporting Information

Ex-situ modification of activated carbon through hydrothermal oxidation and sulphur@amine doping for highly efficient Pb^{2+} sorption: Experimental and modelling approaches

Idris-Hermann TIOTSOP KUETE[1*], Cyrille Ghislain FOTSOP[2], Alexandra LIEB[2], Franziska SCHEFFLER[2*]

[1]Materials and Process Engineering Team, Research Unit of Noxious Chemistry and Environmental Engineering (RUNOCHEE), Department of Chemistry, Faculty of Science, University of Dschang, P.O. Box 67, Dschang, Cameroon

[2]Otto-von-Guericke-University Magdeburg, Chemical Institute, Chair for Industrial Chemistry, Universitätsplatz 2, 39106 Magdeburg, Germany

***** Corresponding author

E-mail address: hermann.kuete90@gmail.com; franziska.scheffler@ovgu.de

Table S1: Central composite design for the adsorption of Pb^{2+} using **ACH-L-Cyst and AC-$KMnO_4$**

N°	pH	Time (min)	Concentration (mg/L)	Mass (mg)
1.	8	5	20	100
2.	5	122.5	210	60
3.	5	122.5	210	60
4.	2	240	400	100
5.	5	240	210	60
6.	5	5	210	60
7.	8	240	400	100
8.	2	240	20	20
9.	5	122.5	210	20
10.	5	122.5	20	60
11.	2	122.5	210	60
12.	5	122.5	210	60
13.	2	5	20	100
14.	2	240	20	100
15.	8	240	400	20
16.	8	5	400	100
17.	2	240	400	20
18.	5	122.5	210	100
19.	5	122.5	210	60
20.	8	5	400	20
21.	8	122.5	210	60
22.	8	240	20	20
23.	2	5	400	20
24.	8	5	20	20
25.	2	5	400	100
26.	8	240	20	100
27.	5	122.5	400	60
28.	2	5	20	20

Table S2: Mathematical kinetics models

Kinetic models	Non-linear forms	References
Pseudo-first order	$Q_t = Q_e(1-e^{-K_1 t})$	[1]
Pseudo-second order	$Q_t = \frac{K_2 Q_e^2 t}{(1+K_2 Q_e t)}$ and h = $K_2 Q_e^2$	[1]
Intraparticle diffusion	$Q_t = K_{\text{int}} t^{\frac{1}{2}} + C$	[2], [3]
Elovich	$Q_t = \frac{1}{\beta}\ln(1+\alpha\beta t)$	[4]

Table S3: Mathematical isotherm models

Parameters	Isotherms	Non-linear forms	References
Two	**Langmuir**	$Q_e = \frac{Q_m K_L C_e}{1+K_L C_e}$	[1], [5]
	Freundlich	$Q_e = K_f C_e^{1/n}$	[1], [5]
	Jovanovic	$Q_e = Q_m(1-e^{-K_J C_e})$	[4]
	Temkin	$Q_e = \frac{RT}{\Delta Q}\ln(ACe)$	[4]
	Dubinin-Radushkevich	$Q_e = Q_m \exp(-\beta\varepsilon^2)$	[5]
Three	**Langmuir-Freundlich**	$Q_e = \frac{Q_{mLF}(K_{LF}C_e)^{M_{LF}}}{1+(K_{LF}C_e)^{M_{LF}}}$	[4]
	Redlich-peterson	$Q_e = \frac{K_{RP}C_e}{1+A_{RP}C_e^g}$	[6]

Langmuir separation factor: $R_L = \frac{1}{1+K_L C_0}$

Table S4: Error functions and their equations

Error function	Abbreviation	formula	References
Residual Root Mean Square Error	**RMSE**	$\sqrt{\frac{1}{n-2}\sum_{i=1}^{N}(Q_{e,\exp}-Q_{e,cal})^2}$	[7]
Chi-square test	**χ^2**	$\sum_{i=1}^{N}\frac{(Q_{e,\exp}-Q_{e,cal})^2}{Q_{e,cal}}$	[7]
Sum Square of Errors	**SCE**	$\sum_{i=1}^{N}(Q_{e,\exp}-Q_{e,cal})_i^2$	[7]
Average Relative Error	**ARE**	$\frac{100}{N}\sum_{i=1}^{N}\left\|\frac{Q_{e,i,cal}-Q_{e,i,\exp}}{Q_{e,i,\exp}}\right\|$	[7]
coefficient of determination	**R^2**	$\frac{\sum_{i=1}^{N}(Q_{e,cal}-Q_{m\exp})^2}{\sum_{i=1}^{N}(Q_{e,cal}-Q_{m\exp})^2+(Q_{e,cal}-Q_{m\exp})^2}$	[7]

Table S5: Model fit and summary statistics for ACH-L-Cyst

Source	Std. Dev.	R^2	Adjusted R^2	Predicted R^2	PRESS	
Linear	17.26	0.2111	0.0739	-0.1301	9810.94	
2FI	16.45	0.4702	0.1585	0.1614	7280.48	
Quadratic	**4.36**	**0.9716**	**0.9410**	**0.7718**	**1981.21**	**Suggested**
Cubic	2.09	0.9975	0.9864	0.6917	2676.86	Aliased

Table S6: Model fit and summary statistics for AC-$KMnO_4$

Source	Std. Dev.	R^2	Adjusted R^2	Predicted R^2	PRESS	
Linear	9.17	0.3319	0.2157	-0.1129	3221.83	
2FI	5.70	0.8090	0.6966	0.6032	1148.71	
Quadratic	**1.85**	**0.9847**	**0.9682**	**0.8905**	**316.86**	**Suggested**
Cubic	1.54	0.9959	0.9779	0.1469	2469.59	Aliased

Table S7: Residual from adsorption of Pb^{2+} ions using the central composite design

Run Order	**pH**	**Time (min)**	**Concentration (mg/L)**	**Mass (mg)**	**Residual ACH-L-Cyst**	**Residual AC-$KMnO_4$**
1	+1	-1	-1	+1	3.60	1.88
2	0	0	0	0	-3.18	-0.72
3	0	0	0	0	0.38	-0.68
4	-1	+1	+1	+1	-0.57	-0.23
5	0	+1	0	0	1.64	0.21
6	0	-1	0	0	-0.57	0.78
7	+1	+1	+1	+1	5.70	-0.68
8	-1	+1	-1	-1	1.44	-0.42
9	0	0	0	-1	0.30	-0.97
10	0	0	-1	0	-1.28	0.84
11	-1	0	0	0	0.23	-0.83
12	0	0	0	0	0.56	-0.99
13	-1	-1	-1	+1	3.00	-3.11
14	-1	+1	-1	+1	0.80	1.86
15	+1	+1	+1	-1	-4.53	1.62
16	+1	-1	+1	+1	-2.97	-1.07
17	-1	+1	+1	-1	-2.33	-0.63
18	0	0	0	+1	0.78	1.96
19	0	0	0	0	-0.99	-0.6
20	+1	-1	+1	-1	0.47	-0.61
21	+1	0	0	0	0.85	1.82
22	+1	+1	-1	-1	4.73	0.07
23	-1	-1	+1	-1	5.34	0.28
24	+1	-1	-1	-1	-0.97	-1.26
25	-1	-1	+1	+1	-3.46	1.17
26	+1	+1	-1	+1	-6.88	-1.78
27	0	0	+1	0	2.35	0.15
28	-1	-1	-1	-1	-4.44	1.93

Table S8: Optimal conditions for adsorption, as well as the predicted and experimental values

	Conditions				% Pb^{2+} removal		
Response	**pH**	**Time (min)**	**Concentration (mg/L)**	**Mass (mg)**	**Predicted value**	**Experimental value**	**Error percentage**
ACH-L-Cyst	5	122.5	210	60	78.82	77.20	1.62
AC-$KMnO_4$	5	122.5	210	60	98.10	97.22	0.88

Table S9: Percentages of Pb^{2+} ion removal by the two adsorbents

	ACH-L-Cyst	AC-$KMnO_4$
Nbr of Cycle	Adsorption rate / %	
1	77.00206	97.47369
2	74.26487	95.9656
3	71.84361	83.78402
4	67.22775	77.69731
5	67.07417	67.78589
6	59.39954	66.97124

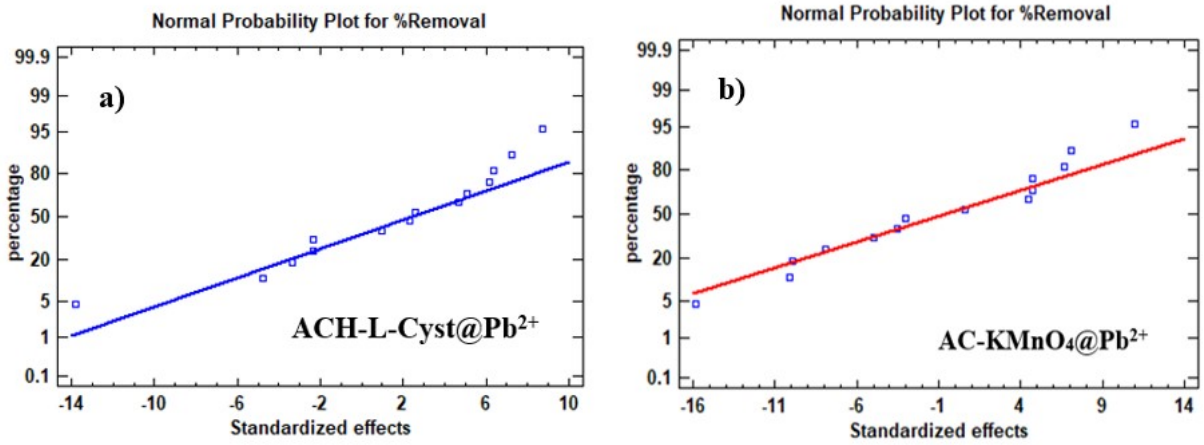

Figure S1 : Normal probability plot for the % Removal of Pb^{2+} adsorbed

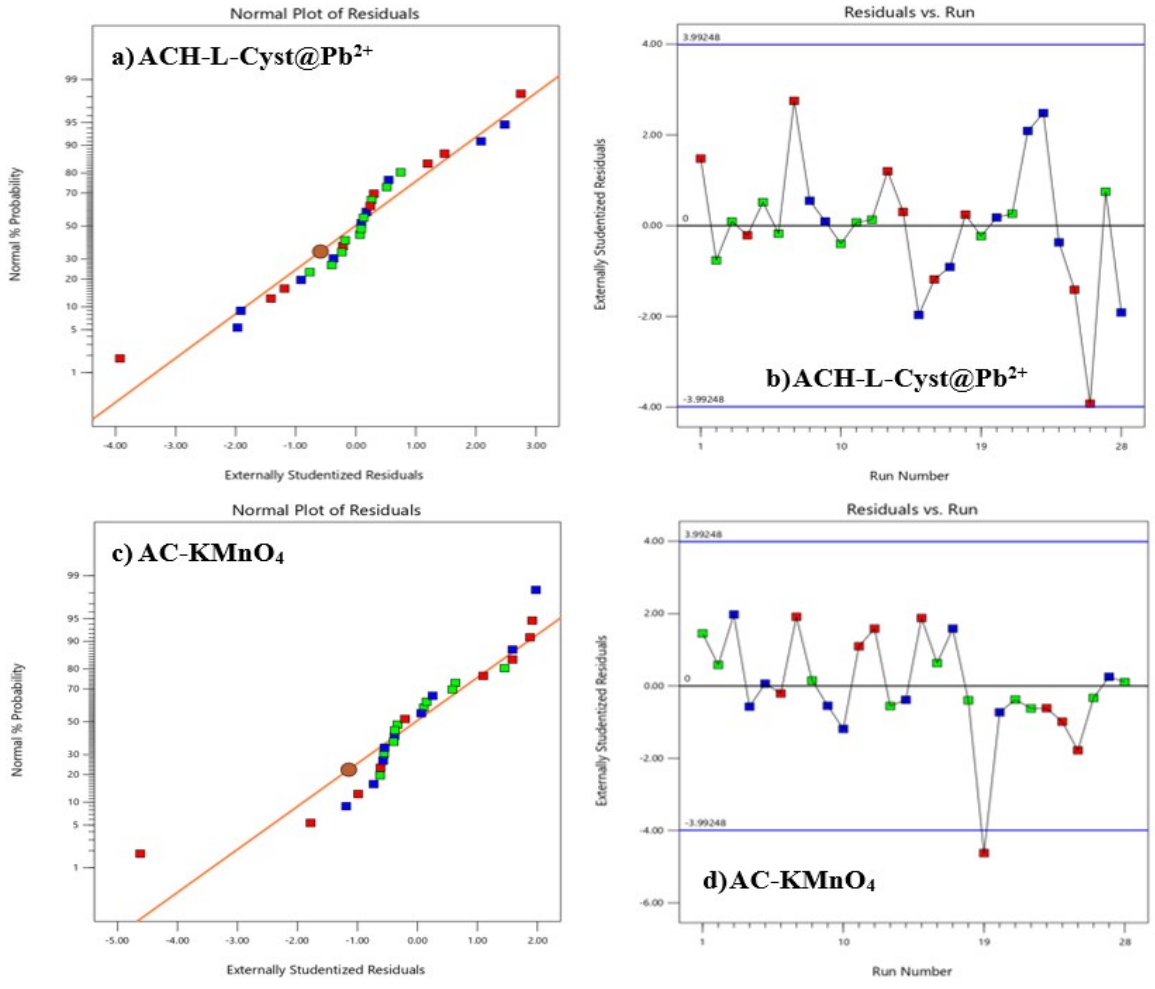

Figure S2 : Normal % probability of residuals (a & c) and externally studentized residuals vs run number for Pb^{2+} ions removal (b & d).

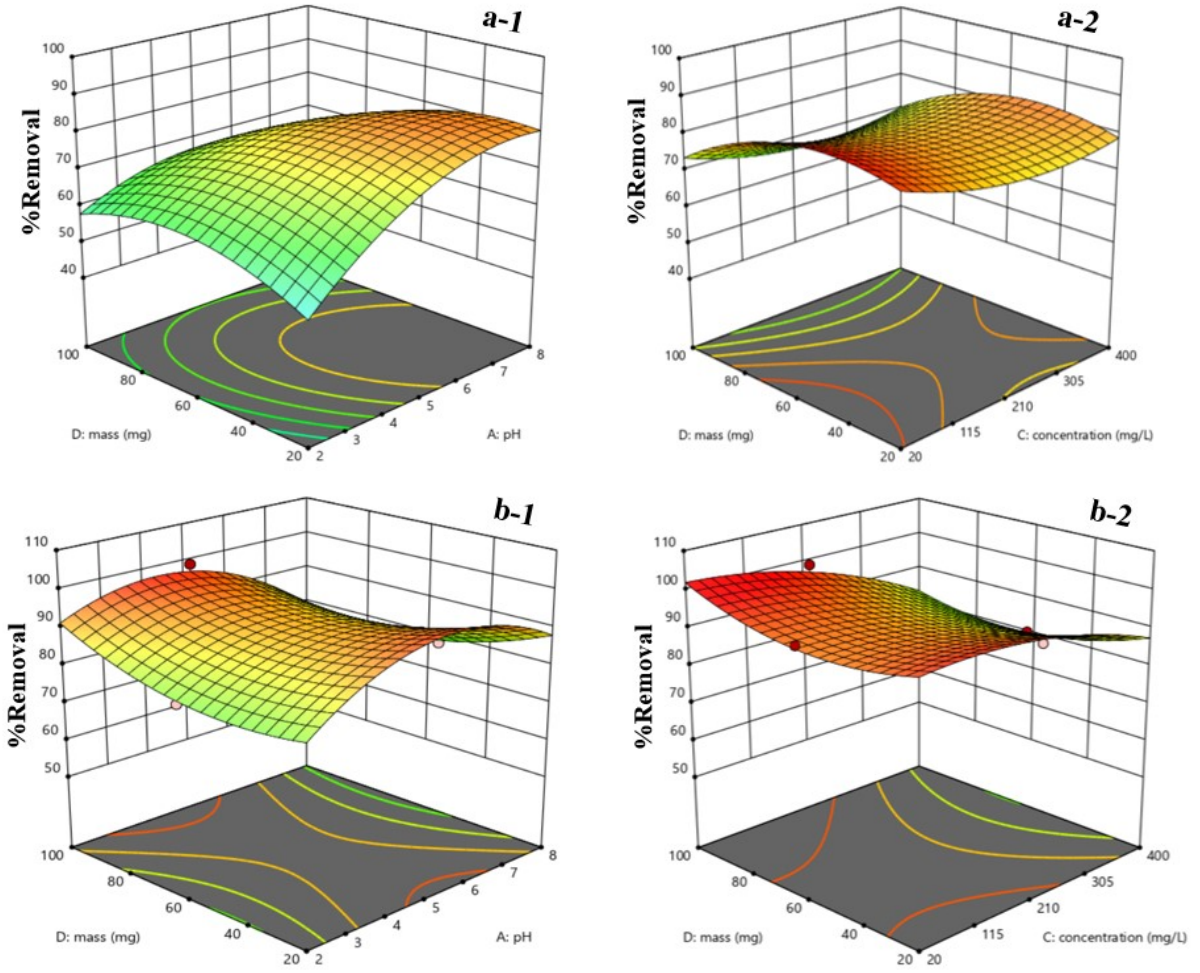

Figure S3 : 3D response surface plots of the CCD showing the effect of pH, concentration (mg/L) and mass (mg) on the adsorption of Pb^{2+} ion (%Removal) using ACH-L-Cyst (a-1 ; a-2) and AC-$KMnO_4$ (b-1 ; b-2)

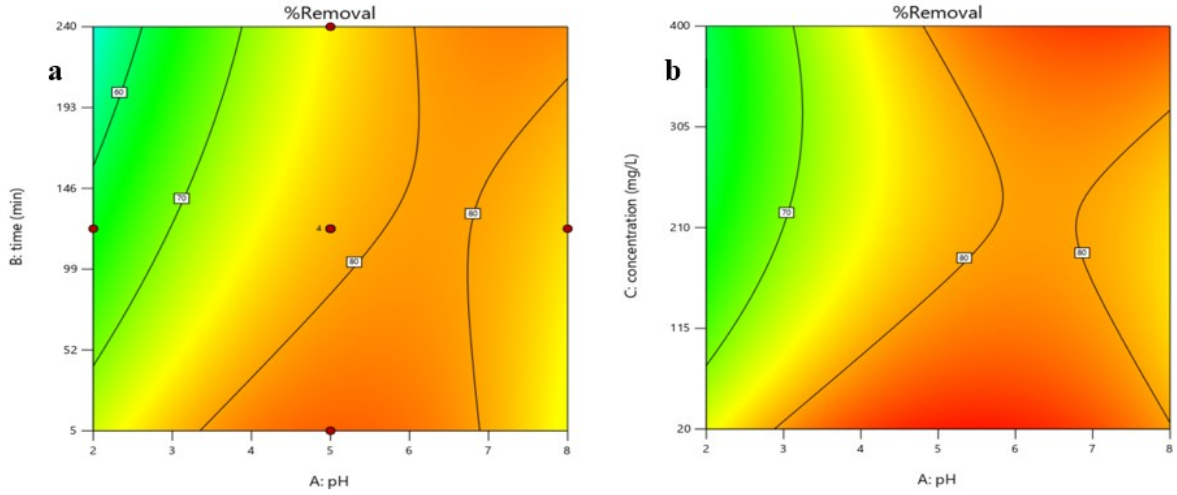

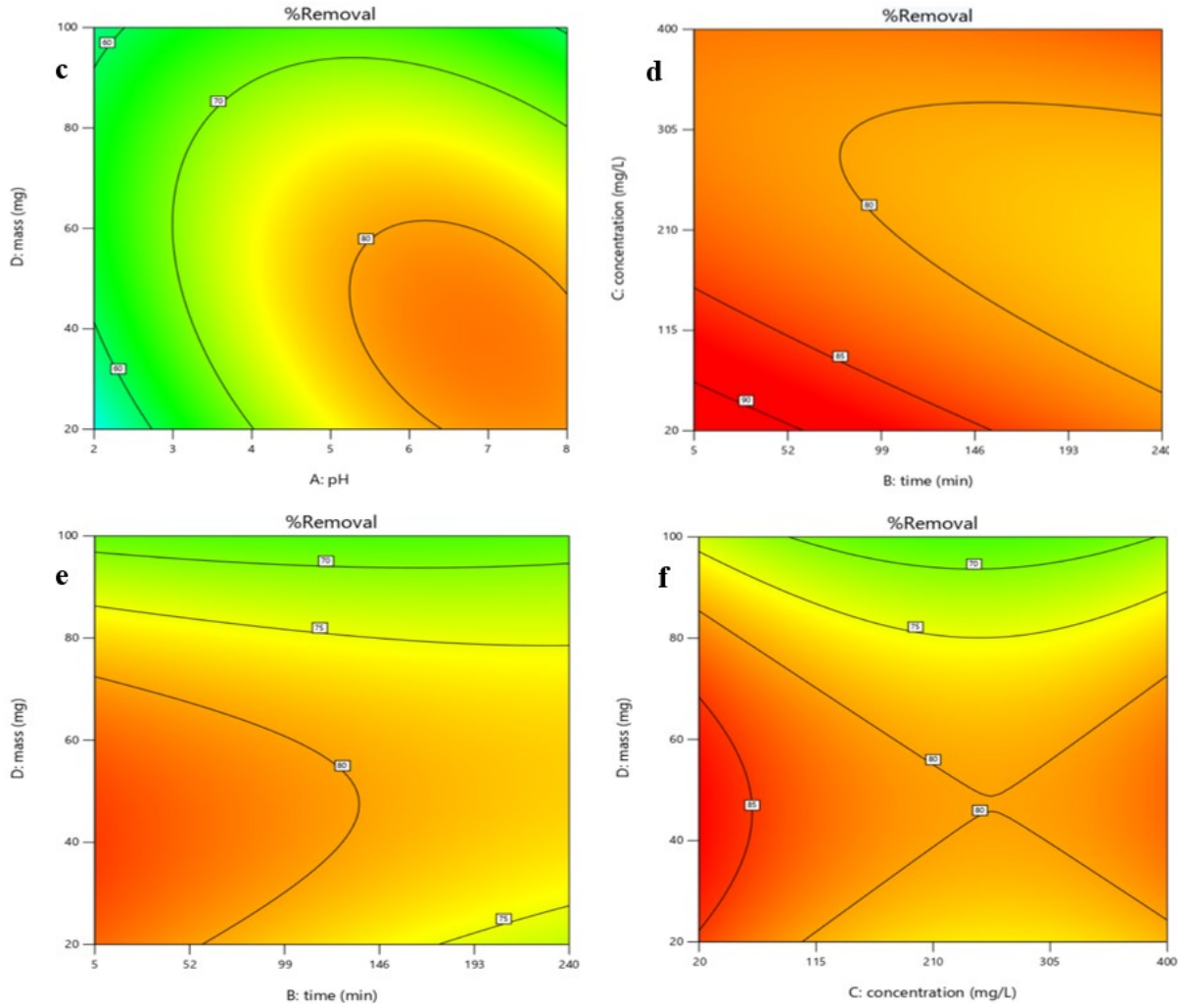

Figure S4 : 2D response surface plots of the CCD showing the effect of pH, time (min), concentration (mg/L) and mass (mg) on the adsorption of the Pb^{2+} (%Removal) using ACH-L-Cyst

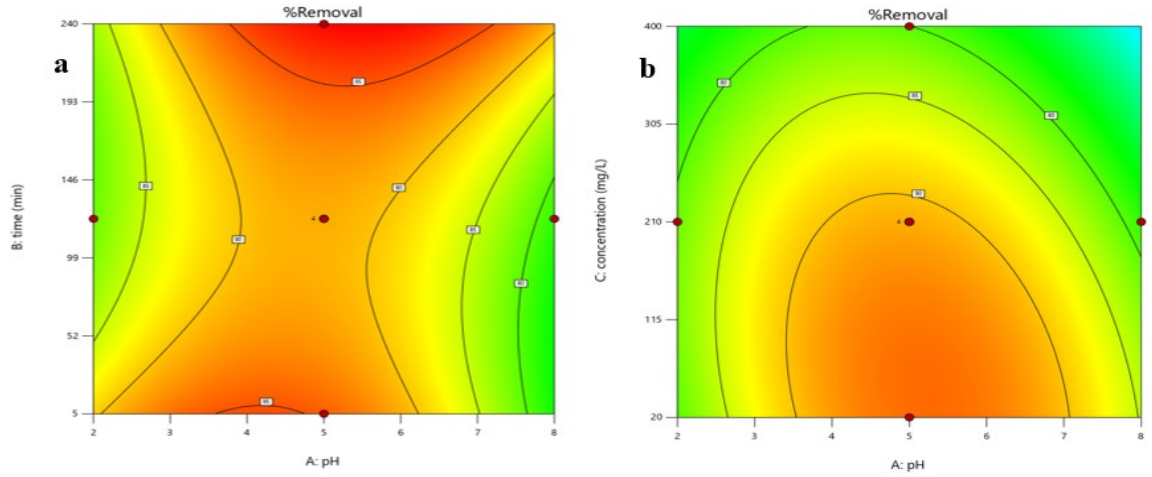

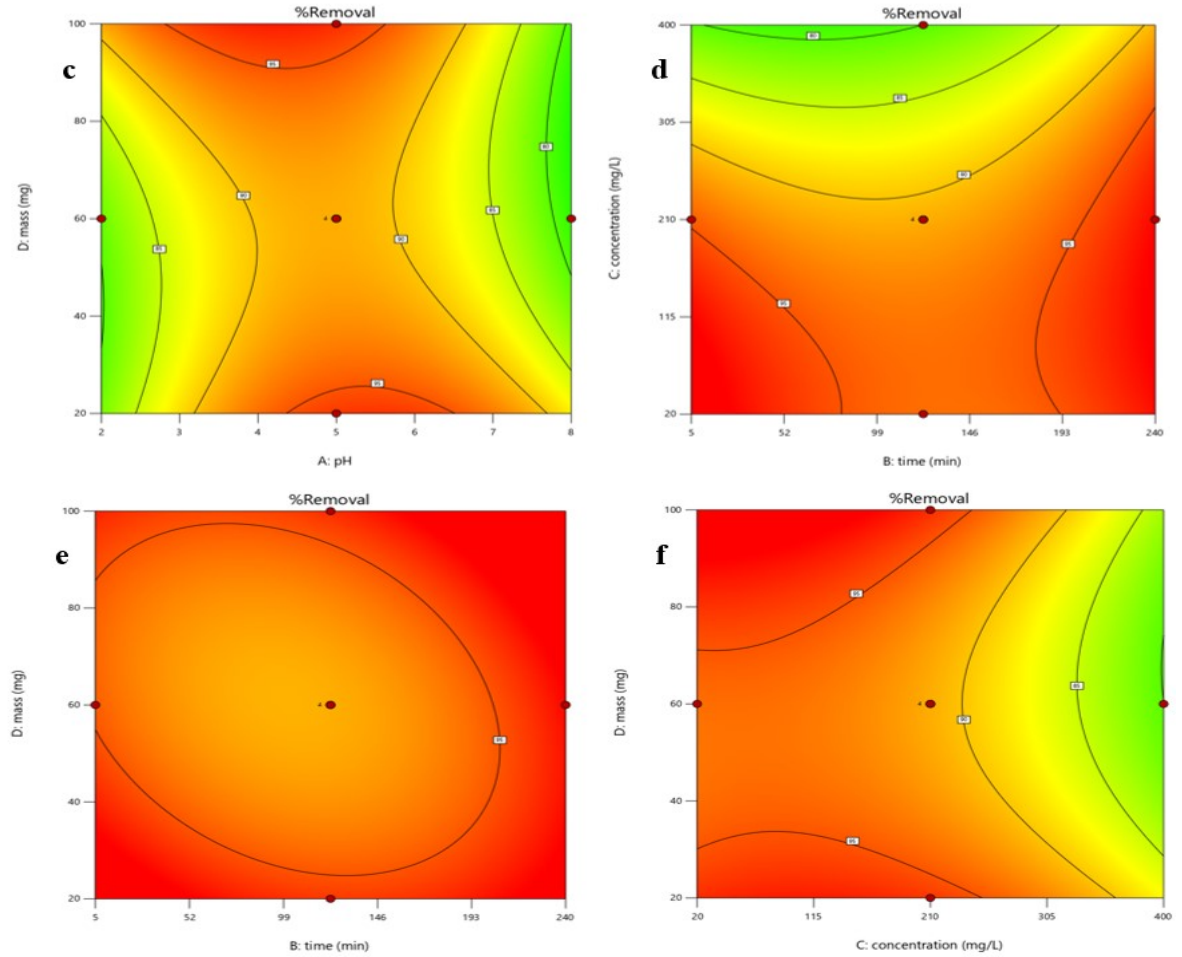

Figure S5 : 2D response surface plots of the CCD showing the effect of pH, time (min), concentration (mg/L) and mass (mg) on the adsorption of the Pb^{2+} (%Removal) using AC-$KMnO_4$

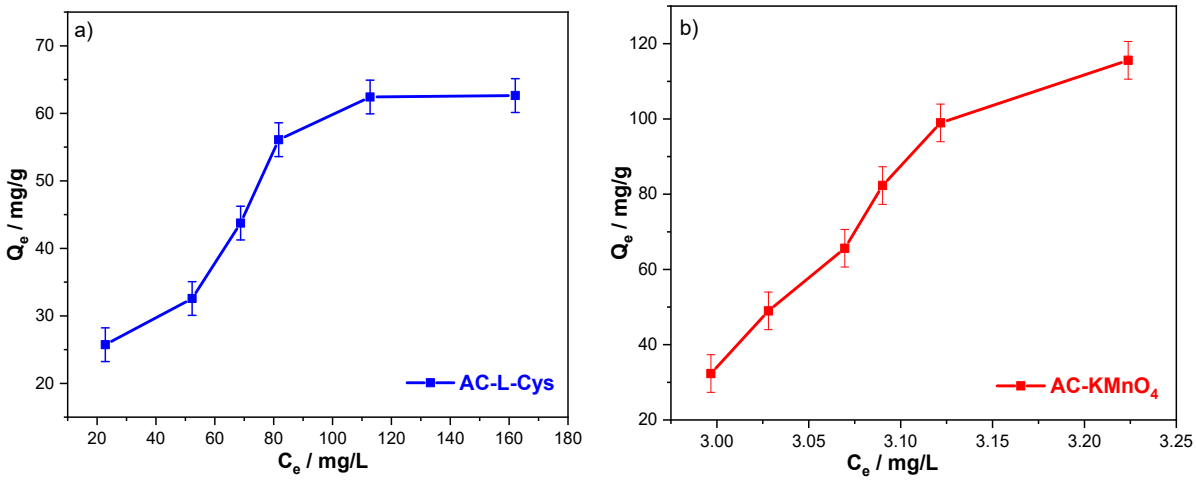

Figure S6 : Impact of concentration on the removal of Pb^{2+} ions by ACH-L-Cyst (a), and AC-$KMnO_4$ (b)

Reference

[1] Y. Liu *et al.*, "Study on the synthesis of poly(pyrrole methane)s with the hydroxyl in different substituent position and their selective adsorption for Pb2+," *Chem. Eng. J.*, 2018, doi: 10.1016/j.cej.2018.12.093.

[2] V. A. Online, "The e ff ective removal of Pb 2 + by activated carbon fi bers modi fi ed by

L -cysteine : exploration of kinetics , thermodynamics and mechanism," pp. 20062–20073, 2022, doi: 10.1039/d2ra01521h.

[3] Z. Lingkai, X. Man, Y. Yuyuan, and L. Ping, "Thiol -functionalized activated carbon fibers as efficient adsorbents," *Mater. Chem. Phys.*, vol. 302, no. November 2022, p. 127552, 2023, doi: 10.1016/j.matchemphys.2023.127552.

[4] I.-H. T. Kuete, D. R. T. Tchuifon, G. N. Ndifor-Angwafor, A. T. Kamdem, and S. G. Anagho, "Kinetic, Isotherm and Thermodynamic Studies of the Adsorption of Thymol Blue onto Powdered Activated Carbons from <i>Garcinia cola Nut</i> Shells Impregnated with H₃PO₄ and KOH: Non-Linear Regression Analysis," *J. Encapsulation Adsorpt. Sci.*, vol. 10, no. 01, pp. 1–27, 2020, doi: 10.4236/jeas.2020.101001.

[5] M. Zbair, "RSC Advances Reusable bentonite clay : modelling and optimization of hazardous lead and p -nitrophenol adsorption using a response surface methodology approach," *RSC Adv.*, vol. 9, pp. 5756–5769, 2019, doi: 10.1039/C9RA00079H.

[6] M. Mushtaq and M. H. Diyanatizadeh, "Jo l P of," *Results Chem.*, no. Vi, p. 102486, 2025, doi: 10.1016/j.rechem.2025.102486.

[7] D. Alvine Loris *et al.*, "Kinetic and Isotherm Studies of the Adsorption Phenacetin onto Two Copper Porous Coordination Compounds: Nonlinear Regression Analysis," *J. Chem.*, vol. 2022, 2022, doi: 10.1155/2022/2828860.